*PONT (Avignon Mai 2023)*

# Curvature effects on the large scale structure of the universe

arXiv:2206.03059, JCAP 2022

**Centre de Physique Théorique (CPT)**
Julien Bel

**Collaborators:**
Louis Perenon (*Lead*)
Christian Marinoni
Roy Maartens
Julien Larena

# Outline

1) Motivation for studying galaxy clustering in curved space

2) Fourier basis in curved space

3) Galaxy clustering in configuration space

4) Results (KLCDM)

5) Conclusions and Prospects

The example of the cosmic microwave background (CMB):

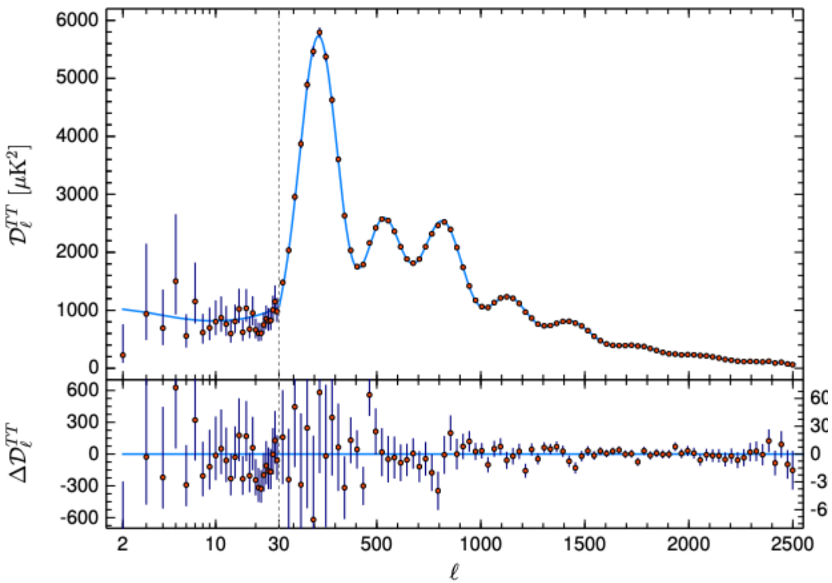


**Fig. 1.** *Planck* 2018 temperature power spectrum. At multipoles $\ell \geq 30$ we show the frequency-coadded temperature computed from the Plik cross-half-mission likelihood, with foreground and other nuisance parameters fixed to a best fit the base-ΛCDM cosmology. In the multipole range $2 \leq \ell \leq 29$, we plot the power spectrum estimates from the Co component-separation algorithm, computed over 86 % of the sky. The base-ΛCDM theoretical spectrum best fit to th TT,TE,EE+lowE+lensing likelihoods is plotted in light blue in the upper panel. Residuals with respect to this model are the lower panel. The error bars show $\pm 1\,\sigma$ diagonal uncertainties, including cosmic variance (approximated as Gaussian, including uncertainties in the foreground model at $\ell \geq 30$. Note that the vertical scale changes at $\ell = 30$, where the horizontal axis switches from logarithmic to linear.

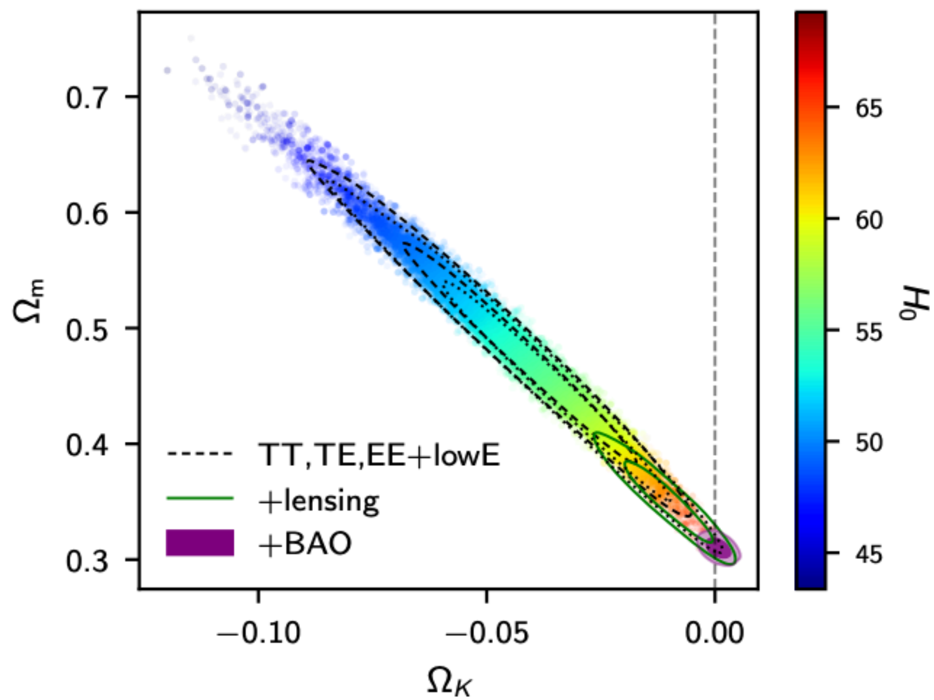


$|\Omega_K| \lesssim 0.1$

$R \approx 9000 h^{-1}\mathrm{Mpc}$

*Planck (2018)*

# Motivation

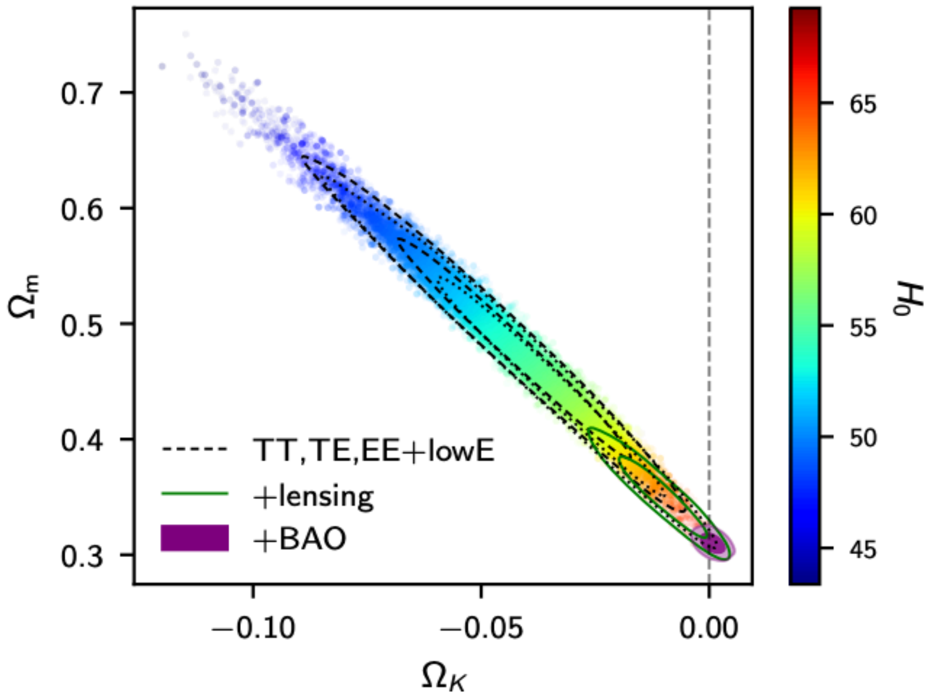


$|\Omega_K| \lesssim 0.1$ $\quad R \approx 9000 h^{-1}\mathrm{Mpc}$

*Planck (2018)*

Euclid typical size:

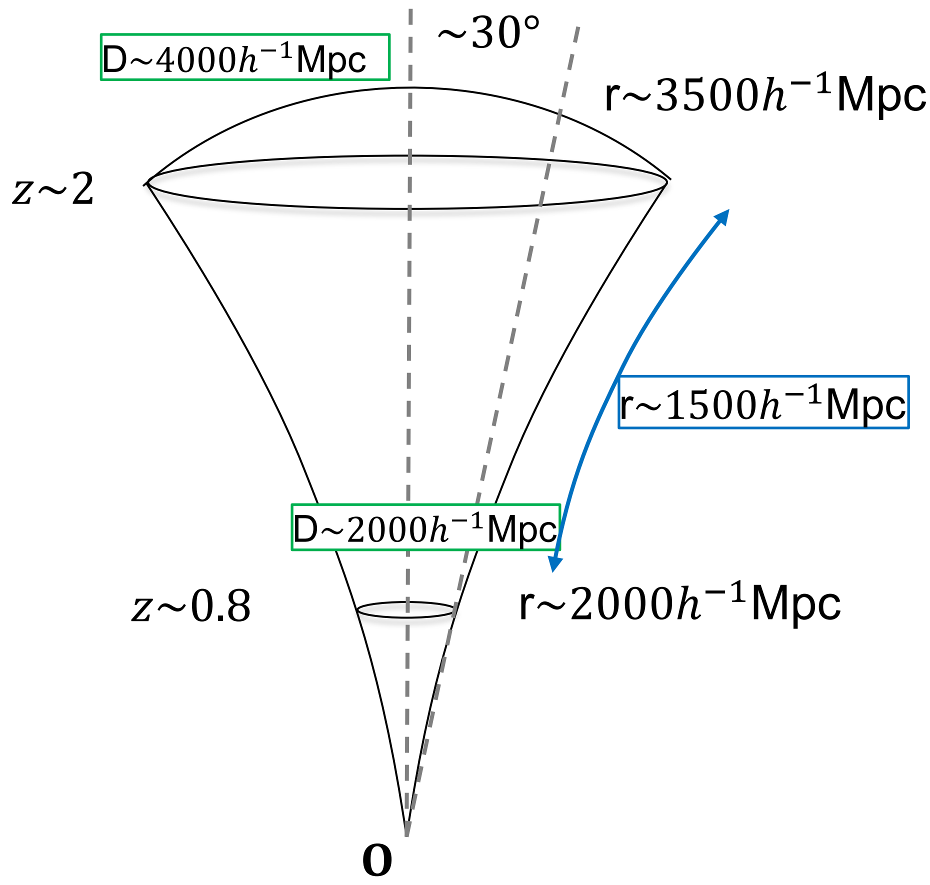


10 to 40 % of curvature scale

## Formalism in curved space

Problem: Fourier basis in curved space ?

FLRW metric:

$$\mathrm{d}s^2 = c^2\,\mathrm{d}t^2 - a^2(t)\,\gamma_{ij}\,\mathrm{d}x^i\,\mathrm{d}x^j = c^2\,\mathrm{d}t^2 - a^2(t)\left[\mathrm{d}\chi^2 + S_K^2(\chi)\left(\mathrm{d}\theta^2 + \sin^2\theta\,\mathrm{d}\phi^2\right)\right]$$

The Fourier basis $\mathcal{Q}$ must be solution of the Helmholtz equation:

$$\tilde{\nabla}^2\mathcal{Q} = \frac{1}{\sqrt{\gamma}}\,\partial_i\left(\sqrt{\gamma}\,\gamma^{ij}\,\partial_j\,\mathcal{Q}\right) = -\tilde{k}^2\mathcal{Q}$$

where $\tilde{\nabla}^2 = a_0^2\,\nabla^2,\ \tilde{k} = a_0\,k$

$$\mathcal{Q}(\chi,\theta,\phi) = R(\chi)Y_{lm}(\theta,\phi)$$

Matsubara (2000)

# Formalism in curved space

Problem: Fourier basis in curved space ?

FLRW metric:

$$ds^2 = c^2\,dt^2 - a^2(t)\,\gamma_{ij}\,dx^i\,dx^j = c^2\,dt^2 - a^2(t)\left[d\chi^2 + S_K^2(\chi)\left(d\theta^2 + \sin^2\theta\,d\phi^2\right)\right]$$

*Temporal part*

The Fourier basis $\mathcal{Q}$ must be solution of the Helmholtz equation:

$$\tilde{\nabla}^2\mathcal{Q} = \frac{1}{\sqrt{\gamma}}\,\partial_i\left(\sqrt{\gamma}\,\gamma^{ij}\,\partial_j\,\mathcal{Q}\right) = -\tilde{k}^2\mathcal{Q}$$

where $\tilde{\nabla}^2 = a_0^2\,\nabla^2,\ \tilde{k} = a_0\,k$

$$\mathcal{Q}(\chi,\theta,\phi) = R(\chi)Y_{lm}(\theta,\phi)$$

Matsubara (2000)

# Formalism in curved space

Problem: Fourier basis in curved space ?

FLRW metric:

$$\mathrm{d}s^2 = c^2\,\mathrm{d}t^2 - a^2(t)\,\gamma_{ij}\,\mathrm{d}x^i\,\mathrm{d}x^j = c^2\,\mathrm{d}t^2 - a^2(t)\left[\mathrm{d}\chi^2 + S_K^2(\chi)\left(\mathrm{d}\theta^2 + \sin^2\theta\,\mathrm{d}\phi^2\right)\right]$$

*Temporal part* ($c^2\,\mathrm{d}t^2$)   *Spatial part* ($a^2(t)\,\gamma_{ij}\,\mathrm{d}x^i\,\mathrm{d}x^j$)

The Fourier basis $\mathcal{Q}$ must be solution of the Helmholtz equation:

$$\tilde{\nabla}^2\mathcal{Q} = \frac{1}{\sqrt{\gamma}}\,\partial_i\left(\sqrt{\gamma}\,\gamma^{ij}\,\partial_j\,\mathcal{Q}\right) = -\tilde{k}^2\mathcal{Q}$$

where $\tilde{\nabla}^2 = a_0^2\,\nabla^2,\ \tilde{k} = a_0\,k$

$$\mathcal{Q}(\chi,\theta,\phi) = R(\chi)Y_{lm}(\theta,\phi)$$

Matsubara (2000)

# Formalism in curved space

Problem: Fourier basis in curved space ?

FLRW metric:

$$\mathrm{d}s^2 = c^2\,\mathrm{d}t^2 - a^2(t)\,\gamma_{ij}\,\mathrm{d}x^i\,\mathrm{d}x^j = c^2\,\mathrm{d}t^2 - a^2(t)\left[\mathrm{d}\chi^2 + S_K^2(\chi)\left(\mathrm{d}\theta^2 + \sin^2\theta\,\mathrm{d}\phi^2\right)\right]$$

*Temporal part* — *Spatial part* — *Radial part*

The Fourier basis $\mathcal{Q}$ must be solution of the Helmholtz equation:

$$\tilde{\nabla}^2\mathcal{Q} = \frac{1}{\sqrt{\gamma}}\partial_i\left(\sqrt{\gamma}\,\gamma^{ij}\,\partial_j\,\mathcal{Q}\right) = -\tilde{k}^2\mathcal{Q}$$

where $\tilde{\nabla}^2 = a_0^2\,\nabla^2,\ \tilde{k} = a_0\,k$

$$\mathcal{Q}(\chi,\theta,\phi) = R(\chi)Y_{lm}(\theta,\phi)$$

Matsubara (2000)

# Formalism in curved space

Problem: Fourier basis in curved space ?

FLRW metric:

$$ds^2 = c^2\,dt^2 - a^2(t)\,\gamma_{ij}\,dx^i\,dx^j = c^2\,dt^2 - a^2(t)\left[d\chi^2 + S_K^2(\chi)\left(d\theta^2 + \sin^2\theta\,d\phi^2\right)\right]$$

Temporal part   Spatial part   Radial part   Angular part

The Fourier basis $\mathcal{Q}$ must be solution of the Helmholtz equation:

$$\tilde{\nabla}^2\mathcal{Q} = \frac{1}{\sqrt{\gamma}}\partial_i\left(\sqrt{\gamma}\,\gamma^{ij}\,\partial_j\,\mathcal{Q}\right) = -\tilde{k}^2\mathcal{Q}$$

where $\tilde{\nabla}^2 = a_0^2\,\nabla^2,\ \tilde{k} = a_0\,k$

$$\mathcal{Q}(\chi,\theta,\phi) = R(\chi)Y_{lm}(\theta,\phi)$$

Matsubara (2000)

# Formalism in curved space

Problem: Fourier basis in curved space ?

FLRW metric:

$$\mathrm{d}s^2 = c^2\,\mathrm{d}t^2 - a^2(t)\,\gamma_{ij}\,\mathrm{d}x^i\,\mathrm{d}x^j = c^2\,\mathrm{d}t^2 - a^2(t)\left[\mathrm{d}\chi^2 + S_K^2(\chi)\left(\mathrm{d}\theta^2 + \sin^2\theta\,\mathrm{d}\phi^2\right)\right]$$

*Temporal part* *Spatial part* *Radial part* *Angular part*

The Fourier basis $\mathcal{Q}$ must be solution of the Helmholtz equation:

$$\tilde{\nabla}^2\mathcal{Q} = \frac{1}{\sqrt{\gamma}}\partial_i\left(\sqrt{\gamma}\,\gamma^{ij}\,\partial_j\,\mathcal{Q}\right) = -\tilde{k}^2\mathcal{Q}$$

where $\tilde{\nabla}^2 = a_0^2\,\nabla^2, \ \tilde{k} = a_0\,k$

$$\mathcal{Q}(\chi,\theta,\phi) = R(\chi)Y_{lm}(\theta,\phi)$$

*Spherical Harmonics*

# Galaxy clustering in configuration space

Redshift space distortions on linear scale:

$$\delta_{\rm g}^s(z,\boldsymbol{r}) = b(z)\delta_{\rm m}(z,\boldsymbol{r}) - \frac{(1+z)}{H(z)}\frac{\partial}{\partial r}\left[\boldsymbol{v}(z,\boldsymbol{r})\cdot\hat{\boldsymbol{r}}\right] - \frac{(1+z)}{H(z)}\alpha(z)\left[\boldsymbol{v}(z,\boldsymbol{r})\cdot\hat{\boldsymbol{r}}\right] + \left[5s(z)-2\right]\kappa(z,\boldsymbol{r}) + \delta_\Phi(z,\boldsymbol{r})$$

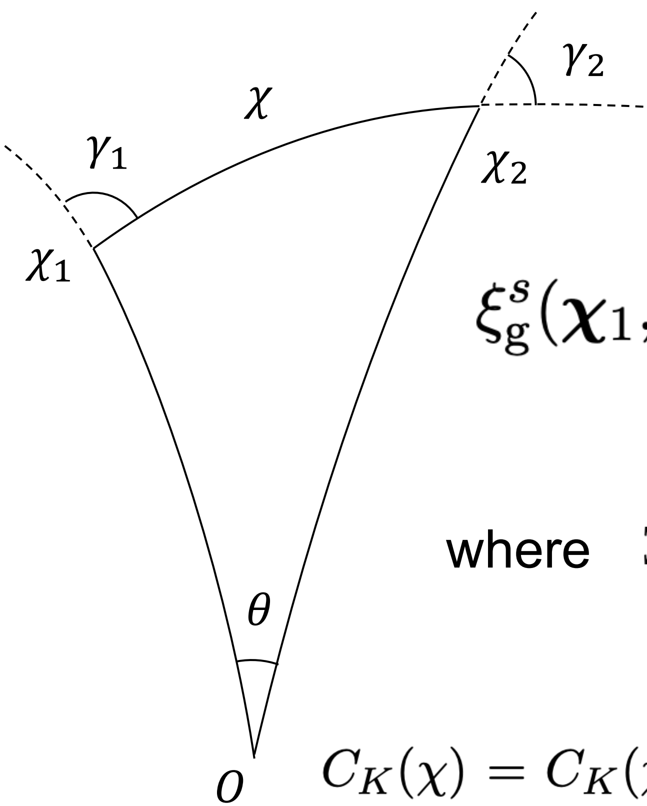


Matsubara (2000)

$$\xi_{\rm g}^s(\boldsymbol{\chi}_1,\boldsymbol{\chi}_2) = b_1 b_2 D_1 D_2 \sum_{n,l} c_l^{(n)}(\chi_1,\chi_2,\theta)\,\Xi_l^{(n)}(\chi)$$

where $\Xi_l^{(n)}(\chi) = 4\pi(-1)^n \int \mathrm{d}\nu\, \frac{\nu^2}{(\nu^2-4K)^n}\mathcal{S}(\nu)X_l^{(K)}(\nu,\chi)$

$$C_K(\chi) = C_K(\chi_1)C_K(\chi_2) + K\,S_K(\chi_1)S_K(\chi_2)\cos\theta$$

# Galaxy clustering in configuration space

Redshift space distortions on linear scale:

$$\delta_{\rm g}^s(z,\boldsymbol{r}) = b(z)\delta_{\rm m}(z,\boldsymbol{r}) - \frac{(1+z)}{H(z)}\frac{\partial}{\partial r}\left[\boldsymbol{v}(z,\boldsymbol{r})\cdot\hat{\boldsymbol{r}}\right] - \frac{(1+z)}{H(z)}\alpha(z)\left[\boldsymbol{v}(z,\boldsymbol{r})\cdot\hat{\boldsymbol{r}}\right] + \left[5s(z)-2\right]\kappa(z,\boldsymbol{r}) + \delta_\Phi(z,\boldsymbol{r})$$

Linear bias

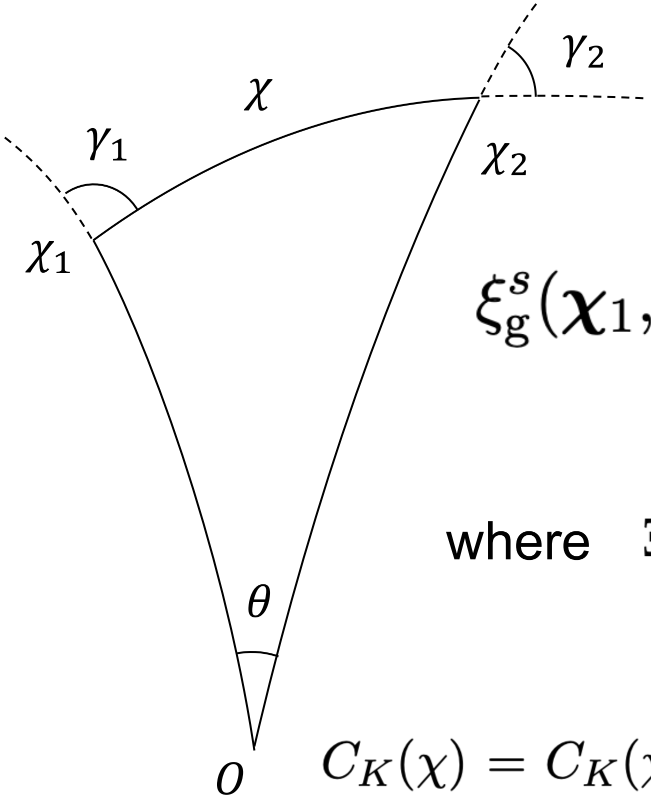


Matsubara (2000)

$$\xi_{\rm g}^s(\boldsymbol{\chi}_1,\boldsymbol{\chi}_2) = b_1 b_2 D_1 D_2 \sum_{n,l} c_l^{(n)}(\chi_1,\chi_2,\theta)\,\Xi_l^{(n)}(\chi)$$

where $\Xi_l^{(n)}(\chi) = 4\pi(-1)^n\int \mathrm{d}\nu\,\frac{\nu^2}{(\nu^2-4K)^n}\mathcal{S}(\nu)X_l^{(K)}(\nu,\chi)$

$$C_K(\chi) = C_K(\chi_1)C_K(\chi_2) + K\,S_K(\chi_1)S_K(\chi_2)\cos\theta$$

# Galaxy clustering in configuration space

Redshift space distortions on linear scale:

Peculiar velocity term

$$\delta^s_{\rm g}(z,\boldsymbol{r}) = b(z)\delta_{\rm m}(z,\boldsymbol{r}) - \frac{(1+z)}{H(z)}\frac{\partial}{\partial r}\left[\boldsymbol{v}(z,\boldsymbol{r})\cdot\hat{\boldsymbol{r}}\right]$$

Linear bias

$$- \frac{(1+z)}{H(z)}\alpha(z)\left[\boldsymbol{v}(z,\boldsymbol{r})\cdot\hat{\boldsymbol{r}}\right] + \left[5s(z)-2\right]\kappa(z,\boldsymbol{r}) + \delta_\Phi(z,\boldsymbol{r})$$

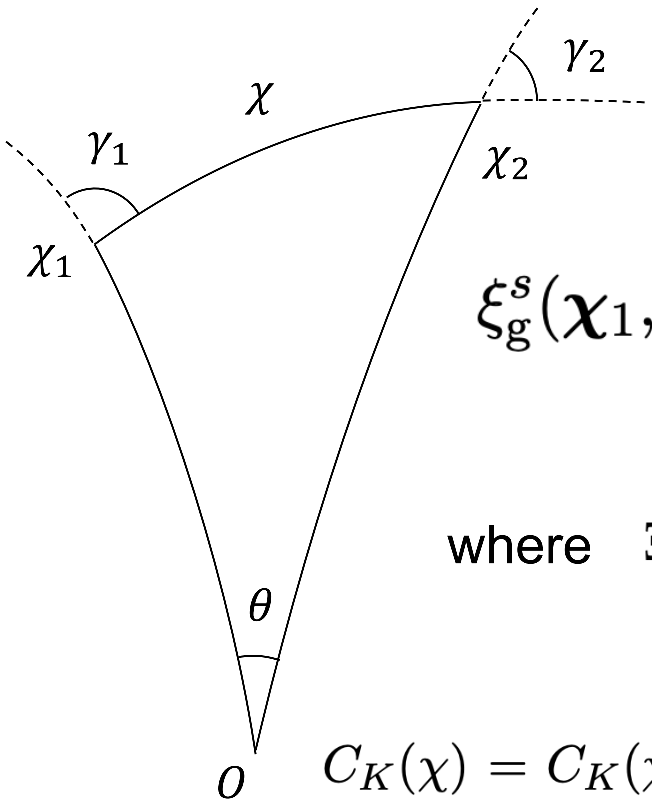


Matsubara (2000)

$$\xi^s_{\rm g}(\boldsymbol{\chi}_1,\boldsymbol{\chi}_2) = b_1 b_2 D_1 D_2 \sum_{n,l} c_l^{(n)}(\chi_1,\chi_2,\theta)\,\Xi_l^{(n)}(\chi)$$

where $\Xi_l^{(n)}(\chi) = 4\pi(-1)^n \int {\rm d}\nu\, \frac{\nu^2}{(\nu^2-4K)^n}\mathcal{S}(\nu)X_l^{(K)}(\nu,\chi)$

$$C_K(\chi) = C_K(\chi_1)C_K(\chi_2) + K\,S_K(\chi_1)S_K(\chi_2)\cos\theta$$

# Galaxy clustering in configuration space

Redshift space distortions on linear scale:

Peculiar velocity term

$$\delta_{\rm g}^s(z,\boldsymbol{r}) = b(z)\delta_{\rm m}(z,\boldsymbol{r}) - \frac{(1+z)}{H(z)}\frac{\partial}{\partial r}\left[\boldsymbol{v}(z,\boldsymbol{r})\cdot\hat{\boldsymbol{r}}\right]$$

Linear bias

$$- \frac{(1+z)}{H(z)}\alpha(z)\left[\boldsymbol{v}(z,\boldsymbol{r})\cdot\hat{\boldsymbol{r}}\right] + \left[5s(z)-2\right]\kappa(z,\boldsymbol{r}) + \delta_\Phi(z,\boldsymbol{r})$$

Relativistic effects

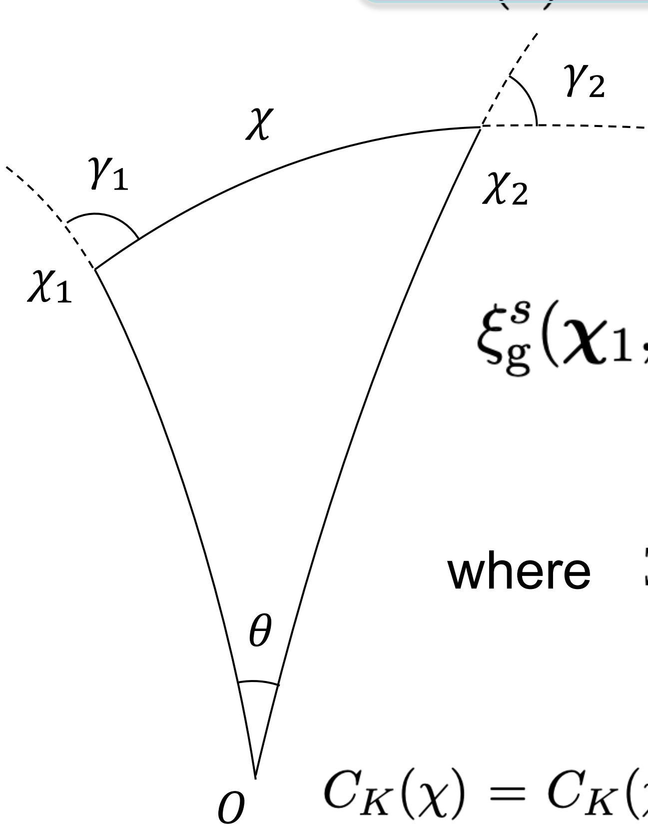


Matsubara (2000)

$$\xi_{\rm g}^s(\boldsymbol{\chi}_1,\boldsymbol{\chi}_2) = b_1 b_2 D_1 D_2 \sum_{n,l} c_l^{(n)}(\chi_1,\chi_2,\theta)\,\Xi_l^{(n)}(\chi)$$

where $\Xi_l^{(n)}(\chi) = 4\pi(-1)^n \int {\rm d}\nu\, \frac{\nu^2}{(\nu^2-4K)^n}\mathcal{S}(\nu)X_l^{(K)}(\nu,\chi)$

$$C_K(\chi) = C_K(\chi_1)C_K(\chi_2) + K\,S_K(\chi_1)S_K(\chi_2)\cos\theta$$

We use galaxy clustering data publicly available:

## Clustering ratio (CR)

$$\eta_R(r) \equiv \frac{\xi_R^{(0)}(r)}{\sigma_R^2}$$

- No bias
- No RSD
- No redshift evolution

It probes the shape of the power spectrum

| Data set | | $z_{\rm min}$ | $z_{\rm max}$ | $\eta_R$ | Ref. |
|---|---|---|---|---|---|
| SDSS | DR7 | 0.15 | 0.43 | 0.096 ± 0.007 | [44, 61] |
| | DR12 | 0.30 | 0.53 | 0.094 ± 0.006 | [44, 62] |
| | DR12 | 0.53 | 0.67 | 0.105 ± 0.011 | [44, 62] |

Bel & Marinoni (2014)
Zennaro et al. (2018)

## $f\sigma_8$ parameter (RSD)

It probes the matter velocity field through anisotropy of the galaxy clustering induced by redshift space distortions

| Data set | $z$ | $f\sigma_8$ | Reference |
|---|---|---|---|
| 2MTF | 0.001 | 0.505 ± 0.085 | [28] |
| 6dFGS+SNIa | 0.02 | 0.428 ± 0.0465 | [29] |
| IRAS+SNIa | 0.02 | 0.398 ± 0.065 | [30, 31] |
| 2MASS | 0.02 | 0.314 ± 0.048 | [31, 32] |
| SDSS | 0.10 | 0.376 ± 0.038 | [33] |
| SDSS-MGS | 0.15 | 0.490 ± 0.145 | [34] |
| 2dFGRS | 0.17 | 0.510 ± 0.060 | [35] |
| GAMA | 0.18 | 0.360 ± 0.090 | [36] |
| GAMA | 0.38 | 0.440 ± 0.060 | [36] |
| SDSS-LRG-200 | 0.25 | 0.3512 ± 0.0583 | [37] |
| SDSS-LRG-200 | 0.37 | 0.4602 ± 0.0378 | [37] |
| BOSS DR12 | 0.31 | 0.469 ± 0.098 | [38] |
| BOSS DR12 | 0.36 | 0.474 ± 0.097 | [38] |
| BOSS DR12 | 0.40 | 0.473 ± 0.086 | [38] |
| BOSS DR12 | 0.44 | 0.481 ± 0.076 | [38] |
| BOSS DR12 | 0.48 | 0.482 ± 0.067 | [38] |
| BOSS DR12 | 0.52 | 0.488 ± 0.065 | [38] |
| BOSS DR12 | 0.56 | 0.482 ± 0.067 | [38] |
| BOSS DR12 | 0.59 | 0.481 ± 0.066 | [38] |
| BOSS DR12 | 0.64 | 0.486 ± 0.070 | [38] |
| WiggleZ | 0.44 | 0.413 ± 0.080 | [39] |
| WiggleZ | 0.60 | 0.390 ± 0.063 | [39] |
| WiggleZ | 0.73 | 0.437 ± 0.072 | [39] |
| Vipers PDR-2 | 0.60 | 0.550 ± 0.120 | [40, 41] |
| Vipers PDR-2 | 0.86 | 0.400 ± 0.110 | [40, 41] |
| FastSound | 1.40 | 0.482 ± 0.116 | [42] |
| SDSS-IV | 0.978 | 0.379 ± 0.176 | [43] |
| SDSS-IV | 1.23 | 0.385 ± 0.099 | [43] |
| SDSS-IV | 1.526 | 0.342 ± 0.070 | [43] |
| SDSS-IV | 1.944 | 0.364 ± 0.106 | [43] |

**-> Alcock-Paczynski**

## Cosmological constraints on KLCDM models:

| Parameter | Prior |
|---|---|
| $\Omega_{b,0}h^2$ | $[0,\ 100]$ |
| $\Omega_{c,0}h^2$ | $[0,\ 100]$ |
| $H_0$ | $[40,\ 100]$ |
| $\tau$ | $[0,\ 0.2]$ |
| $\ln(10^{10}A_s)$ | $[0,\ 100]$ |
| $n_s$ | $[0.9,\ 1]$ |
| $\Omega_{K,0}$ | $[-0.2,\ 0.6]$ |
| $\Omega_{b,0}h^2$ | $\mathcal{N}\left(0.0222, 0.0005^2\right)$ |
| $\sigma_{8,0}$ | $[0.6,\ 1]$ |
| $\Omega_{m,0}$ | $[0,\ 1]$ |

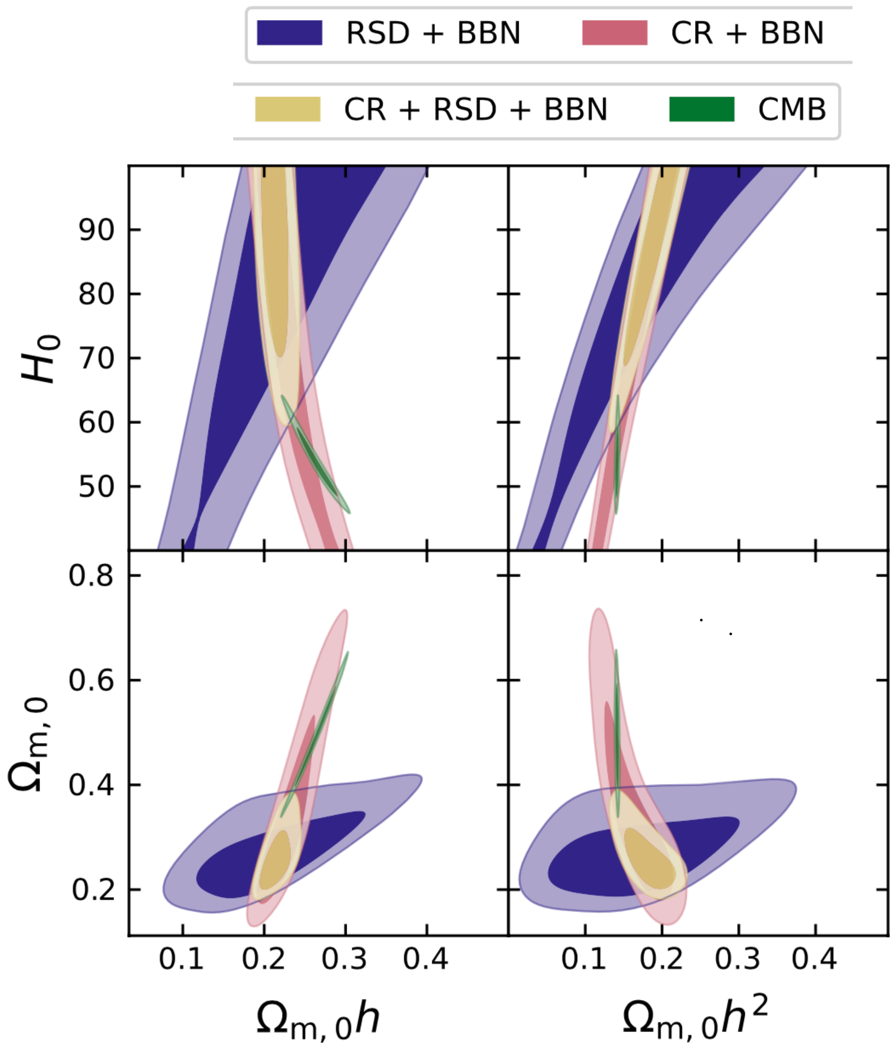

Cosmological constraints on KLCDM models:

| Parameter | Prior |
|---|---|
| $\Omega_{b,0}h^2$ | $[0,\ 100]$ |
| $\Omega_{c,0}h^2$ | $[0,\ 100]$ |
| $H_0$ | $[40,\ 100]$ |
| $\tau$ | $[0,\ 0.2]$ |
| $\ln(10^{10}A_s)$ | $[0,\ 100]$ |
| $n_s$ | $[0.9,\ 1]$ |
| $\Omega_{K,0}$ | $[-0.2,\ 0.6]$ |
| $\Omega_{b,0}h^2$ | $\mathcal{N}\left(0.0222, 0.0005^2\right)$ |
| $\sigma_{8,0}$ | $[0.6,\ 1]$ |
| $\Omega_{m,0}$ | $[0,\ 1]$ |

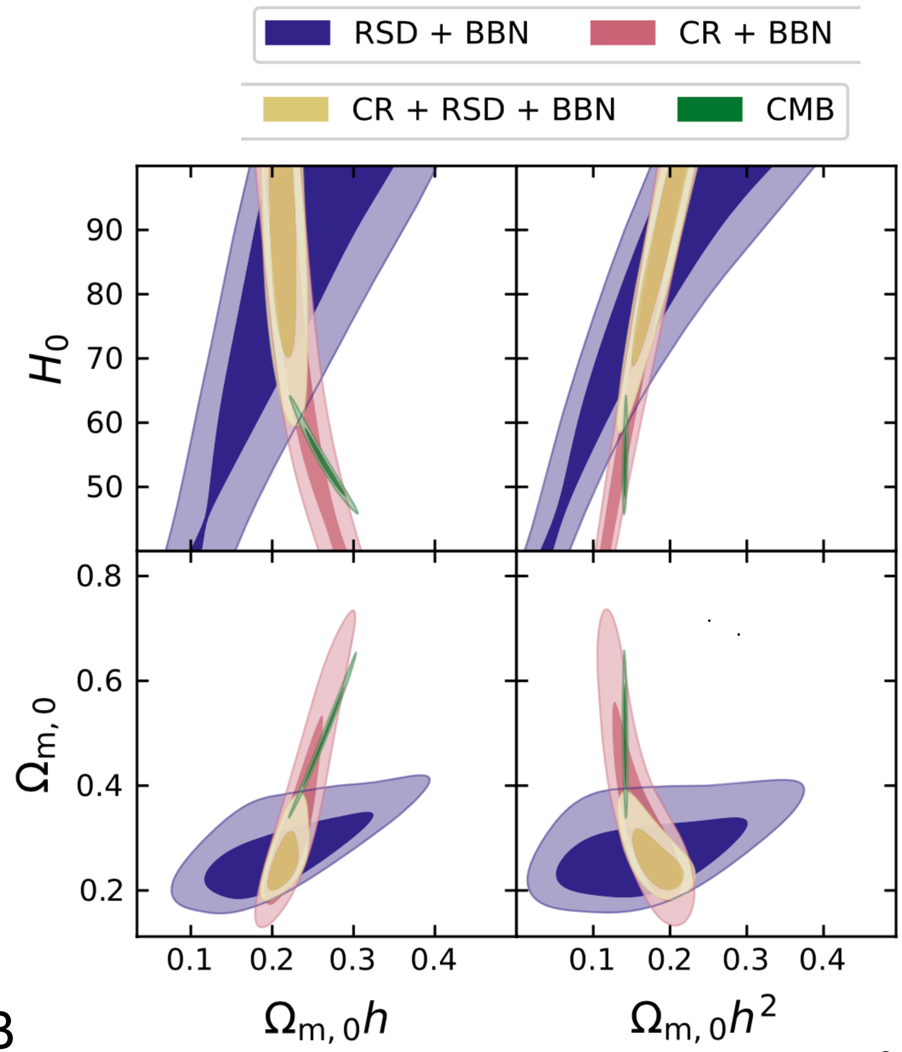


$H_0$ ( > 62 km/s/Mpc at 95% C.L. )

-> completely independent from CMB

# Results

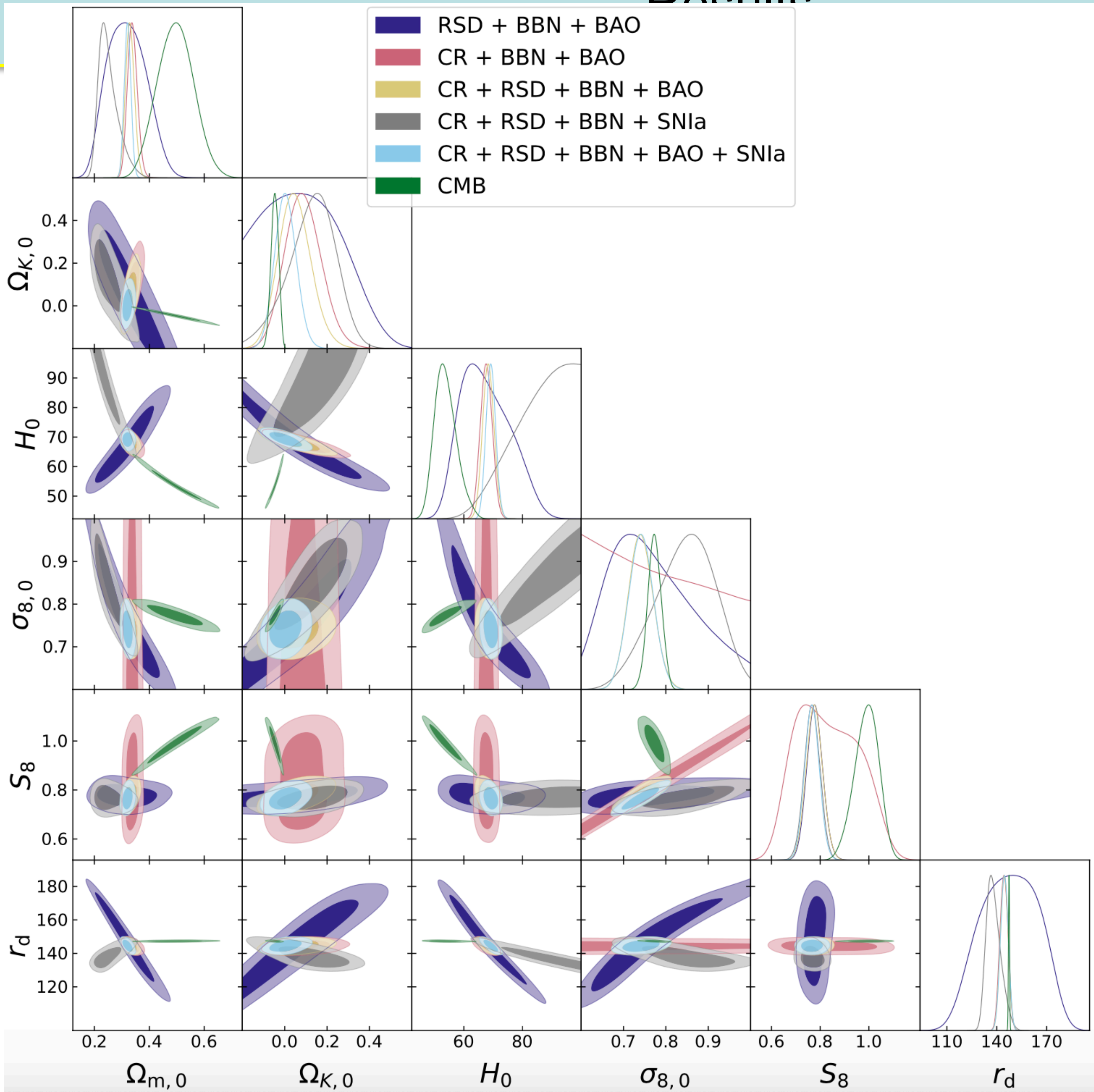
RSD + BBN + BAO
CR + BBN + BAO
CR + RSD + BBN + BAO
CR + RSD + BBN + SNIa
CR + RSD + BBN + BAO + SNIa
CMB
$\Omega_{m,0}$
$\Omega_{K,0}$
$H_0$
$\sigma_{8,0}$
$S_8$
$r_d$

# Deviance Information Criterion (DIC)

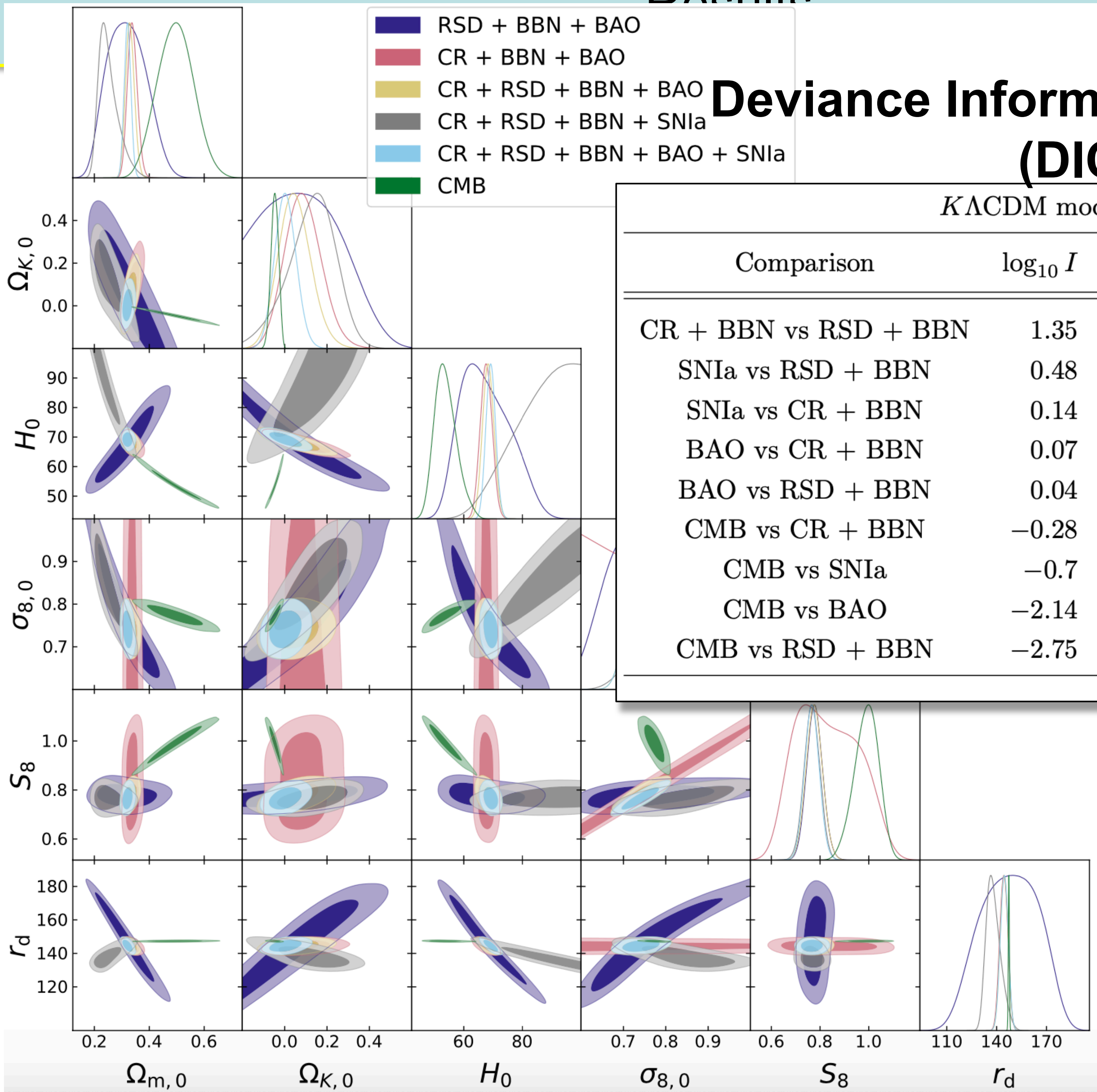


$K\Lambda$CDM model

| Comparison | $\log_{10} I$ | Agreement / Disagreement |
|---|---|---|
| CR + BBN vs RSD + BBN | 1.35 | strong agreement |
| SNIa vs RSD + BBN | 0.48 | inconclusive |
| SNIa vs CR + BBN | 0.14 | inconclusive |
| BAO vs CR + BBN | 0.07 | inconclusive |
| BAO vs RSD + BBN | 0.04 | inconclusive |
| CMB vs CR + BBN | −0.28 | inconclusive |
| CMB vs SNIa | −0.7 | substantial |
| CMB vs BAO | −2.14 | decisive disagreement |
| CMB vs RSD + BBN | −2.75 | decisive disagreement |

# Results

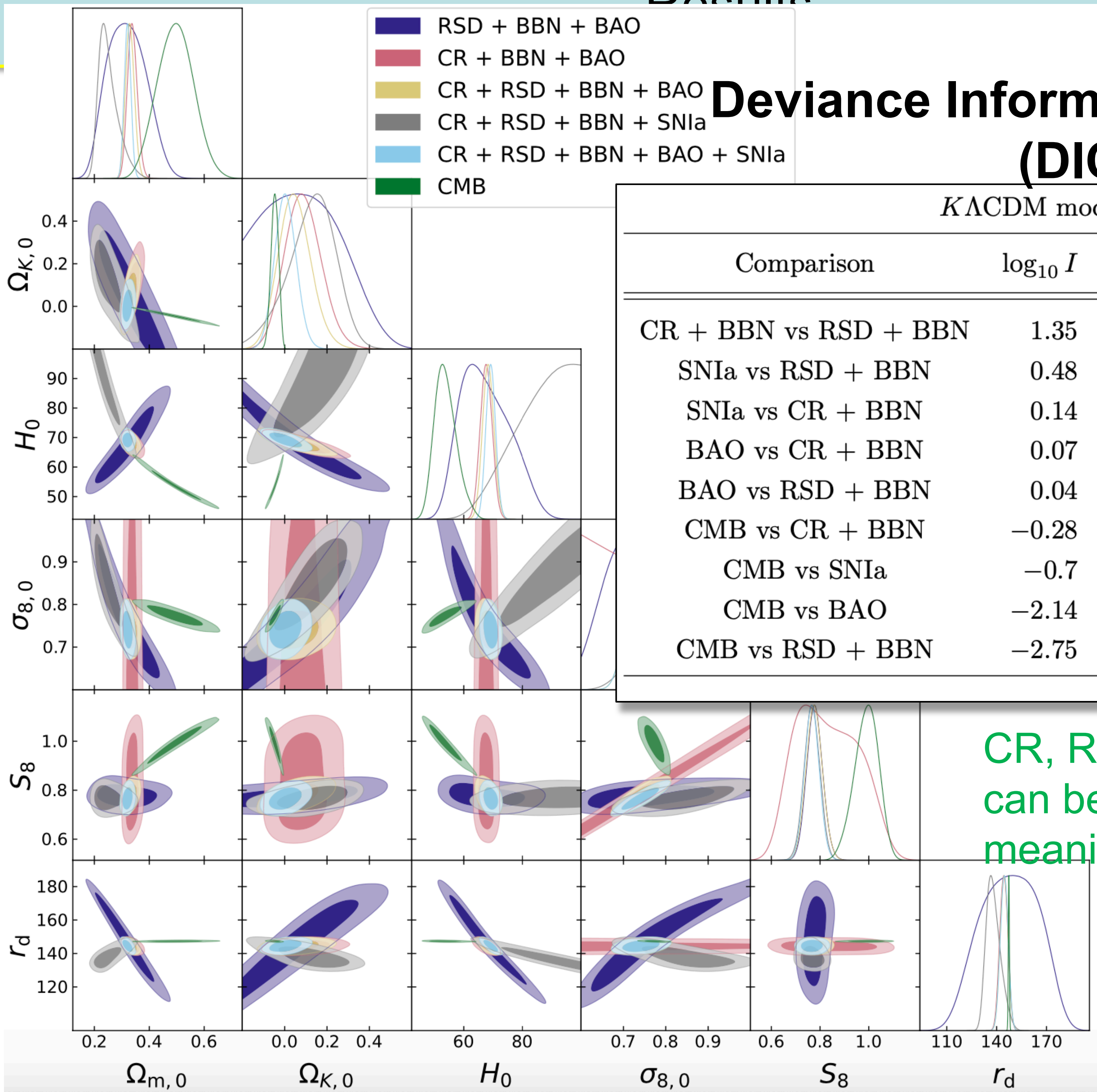


## Deviance Information Criterion (DIC)

$K\Lambda$CDM model

| Comparison | $\log_{10} I$ | Agreement / Disagreement |
|---|---|---|
| CR + BBN vs RSD + BBN | 1.35 | strong agreement |
| SNIa vs RSD + BBN | 0.48 | inconclusive |
| SNIa vs CR + BBN | 0.14 | inconclusive |
| BAO vs CR + BBN | 0.07 | inconclusive |
| BAO vs RSD + BBN | 0.04 | inconclusive |
| CMB vs CR + BBN | −0.28 | inconclusive |
| CMB vs SNIa | −0.7 | substantial |
| CMB vs BAO | −2.14 | decisive disagreement |
| CMB vs RSD + BBN | −2.75 | decisive disagreement |

CR, RSD, BAO and SNIa can be combined in a meaningful way

# Results

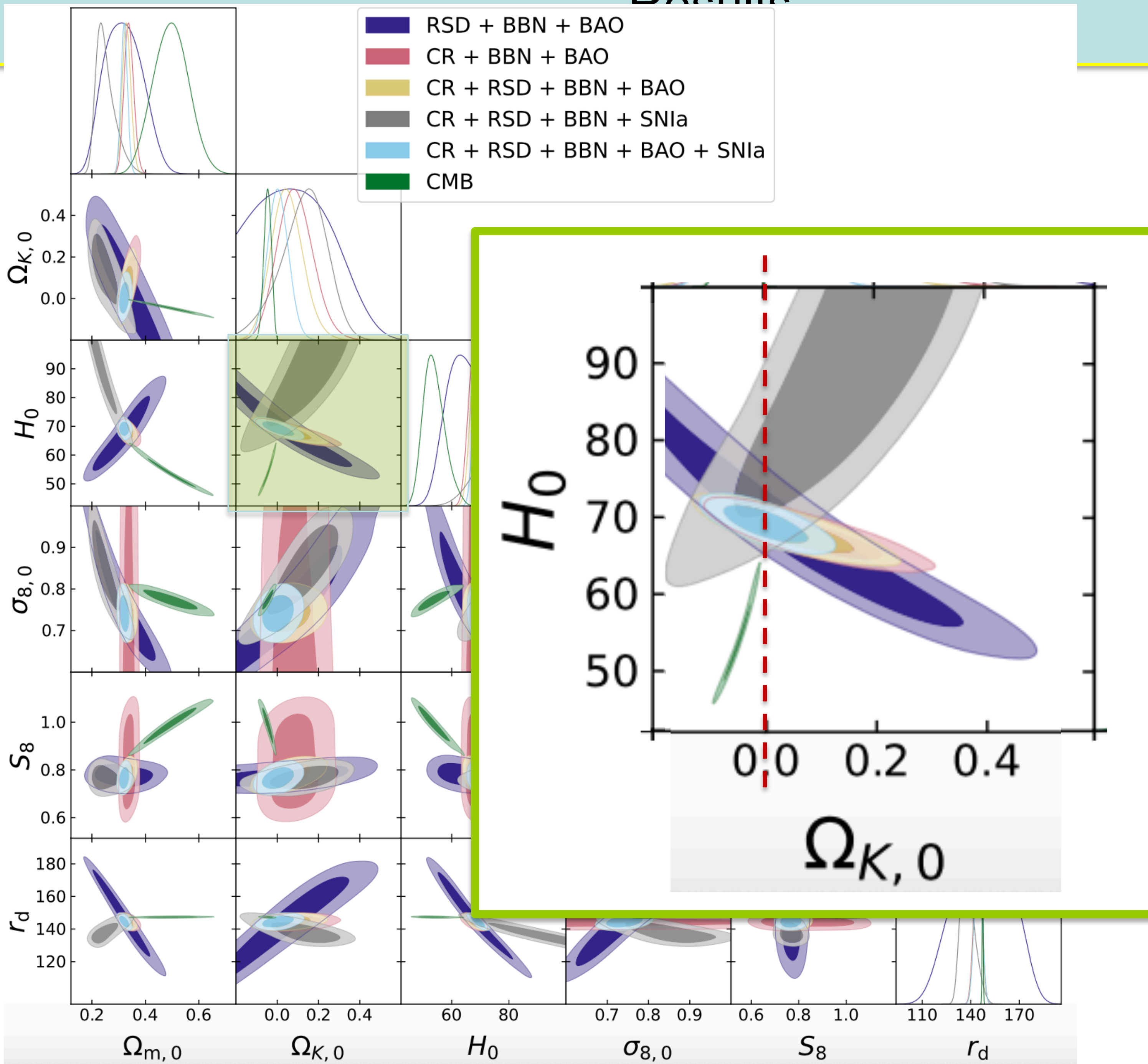
RSD + BBN + BAO
CR + BBN + BAO
CR + RSD + BBN + BAO
CR + RSD + BBN + SNIa
CR + RSD + BBN + BAO + SNIa
CMB
$\Omega_{m,0}$
$\Omega_{K,0}$
$H_0$
$\sigma_{8,0}$
$S_8$
$r_d$
0.2 0.4 0.6
0.0 0.2 0.4
60 80
0.7 0.8 0.9
0.6 0.8 1.0
110 140 170
90 80 70 60 50

# Results

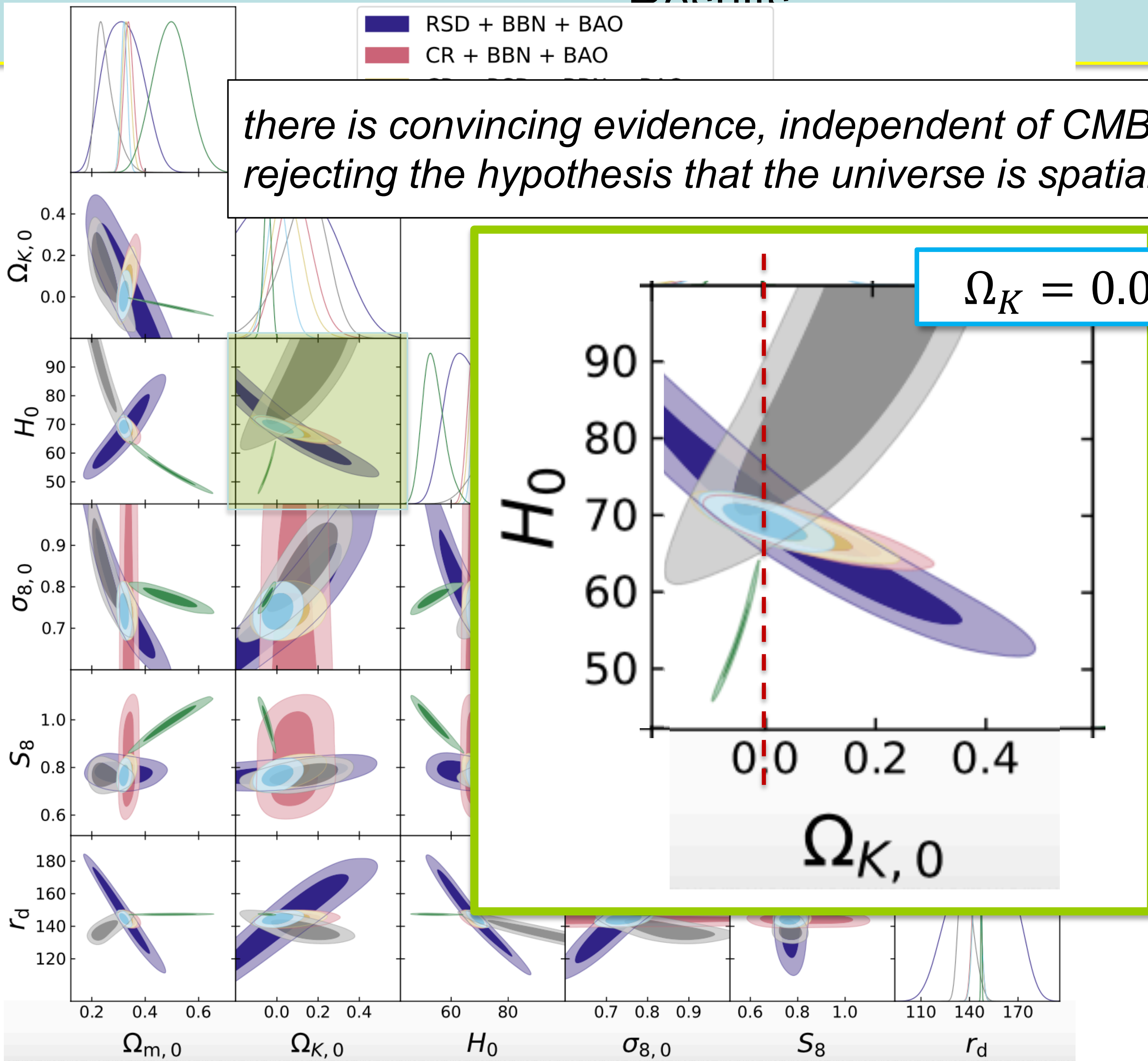


*there is convincing evidence, independent of CMB data, for not rejecting the hypothesis that the universe is spatially flat*

$$\Omega_K = 0.004 \pm 0.05$$

# Results

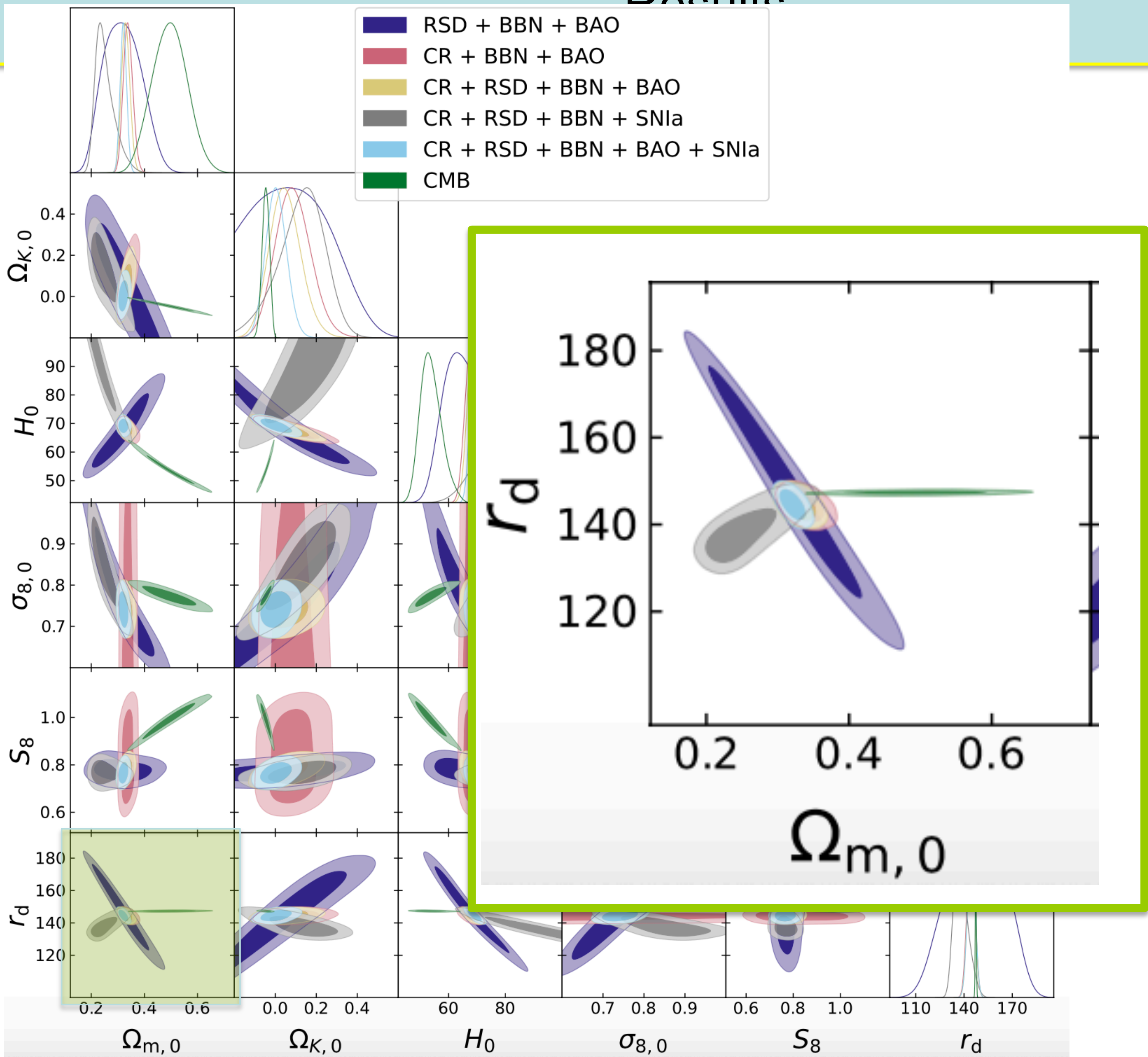

RSD + BBN + BAO
CR + BBN + BAO
CR + RSD + BBN + BAO
CR + RSD + BBN + SNIa
CR + RSD + BBN + BAO + SNIa
CMB
$\Omega_{K,0}$
$H_0$
$\sigma_{8,0}$
$S_8$
$r_d$
$\Omega_{m,0}$

# Results

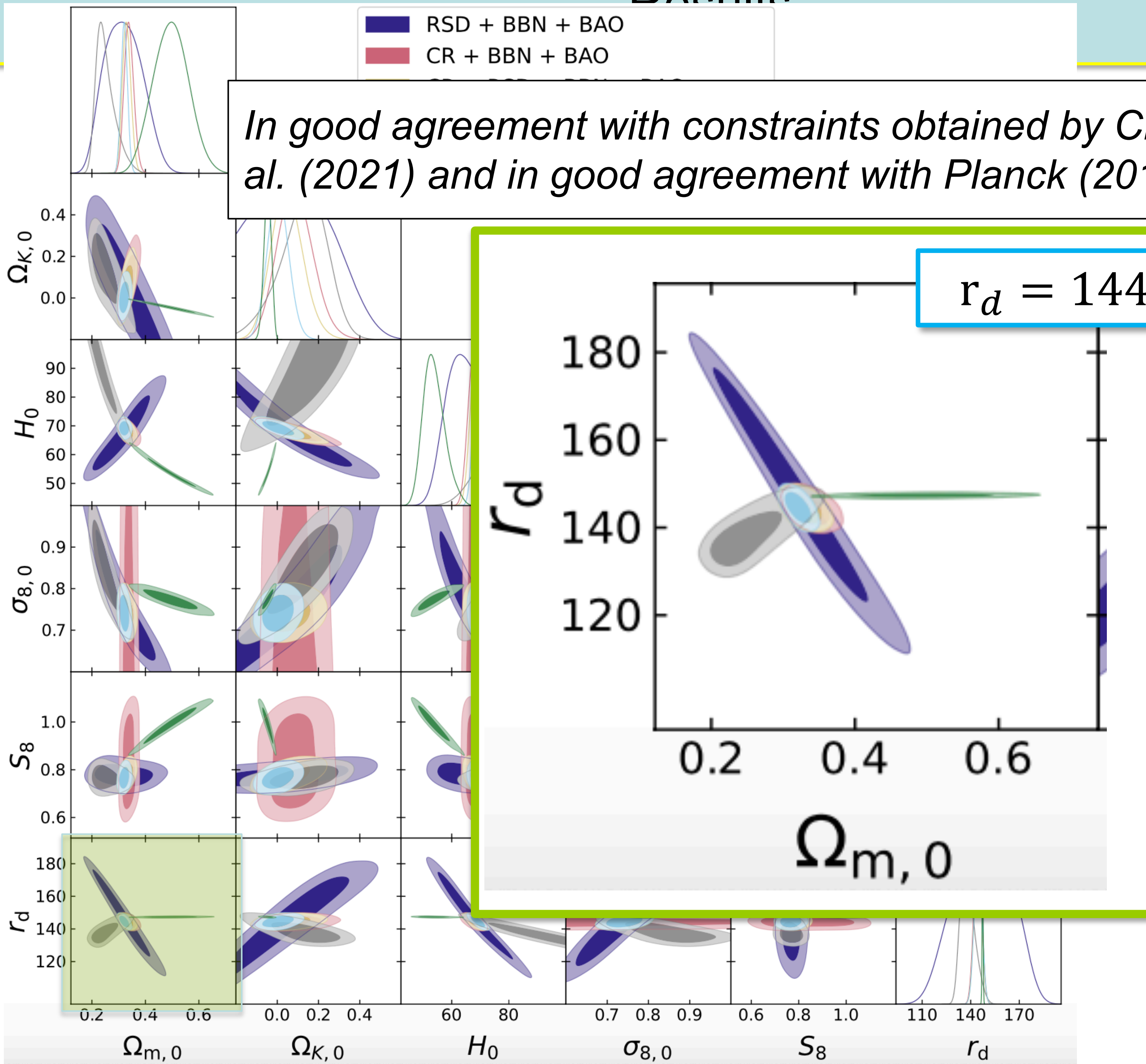


*In good agreement with constraints obtained by Chudaykin et al. (2021) and in good agreement with Planck (2018)*

$r_d = 144.57 \pm 2.34$

( Mpc )

# Results

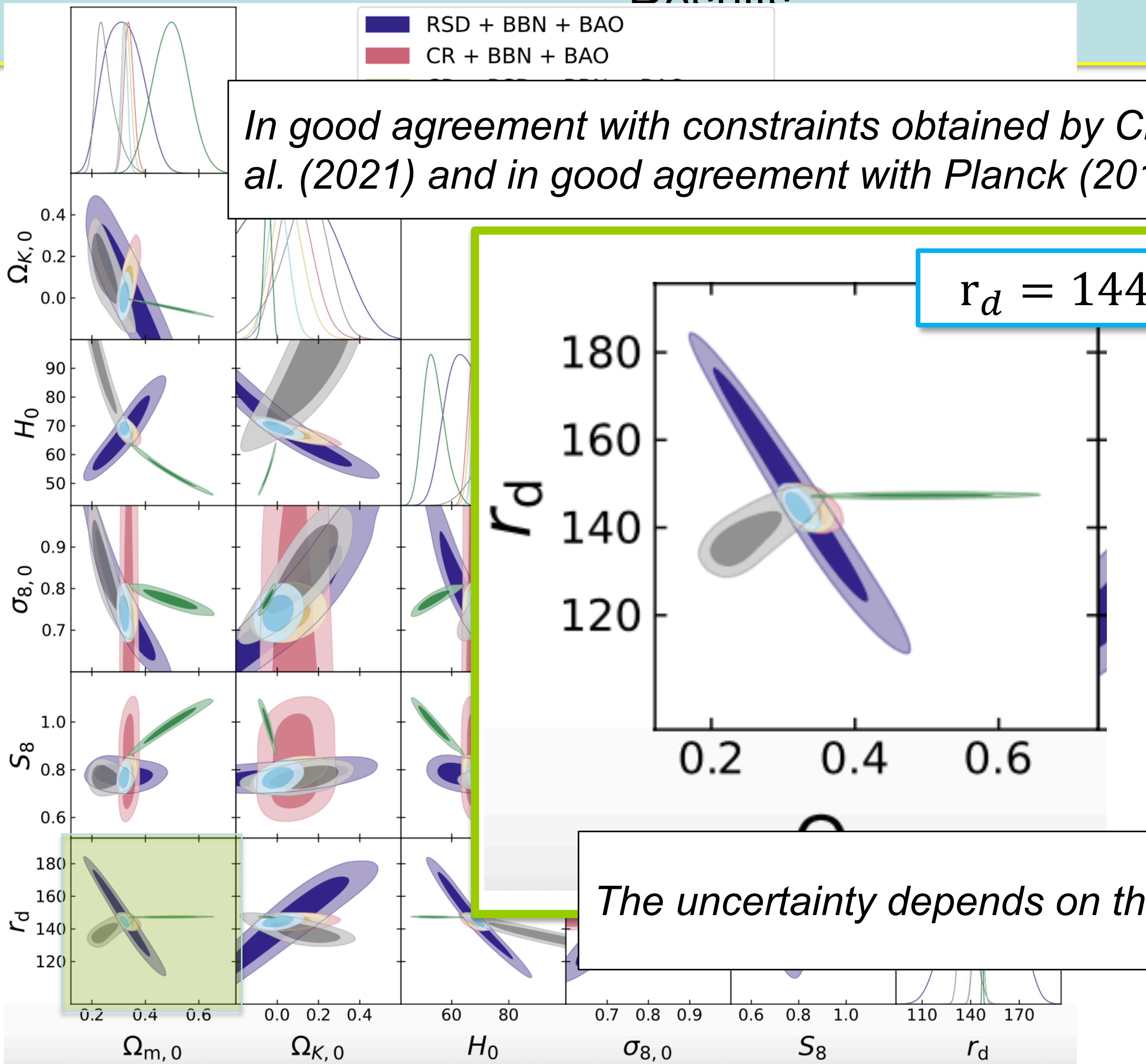


*In good agreement with constraints obtained by Chudaykin et al. (2021) and in good agreement with Planck (2018)*

$r_d = 144.57 \pm 2.34$

( Mpc )

*The uncertainty depends on the BBN prior*

# Results

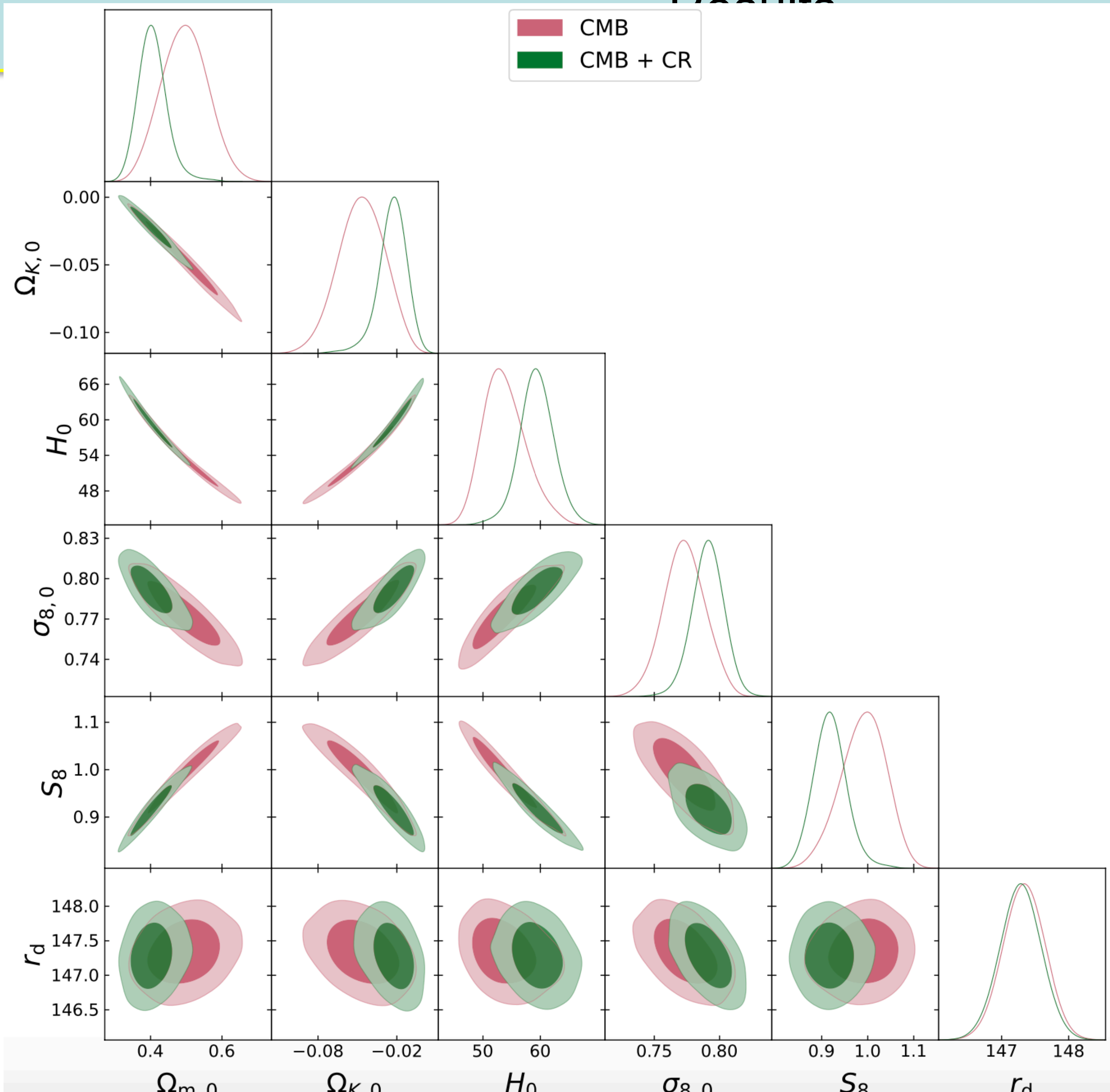

# Results

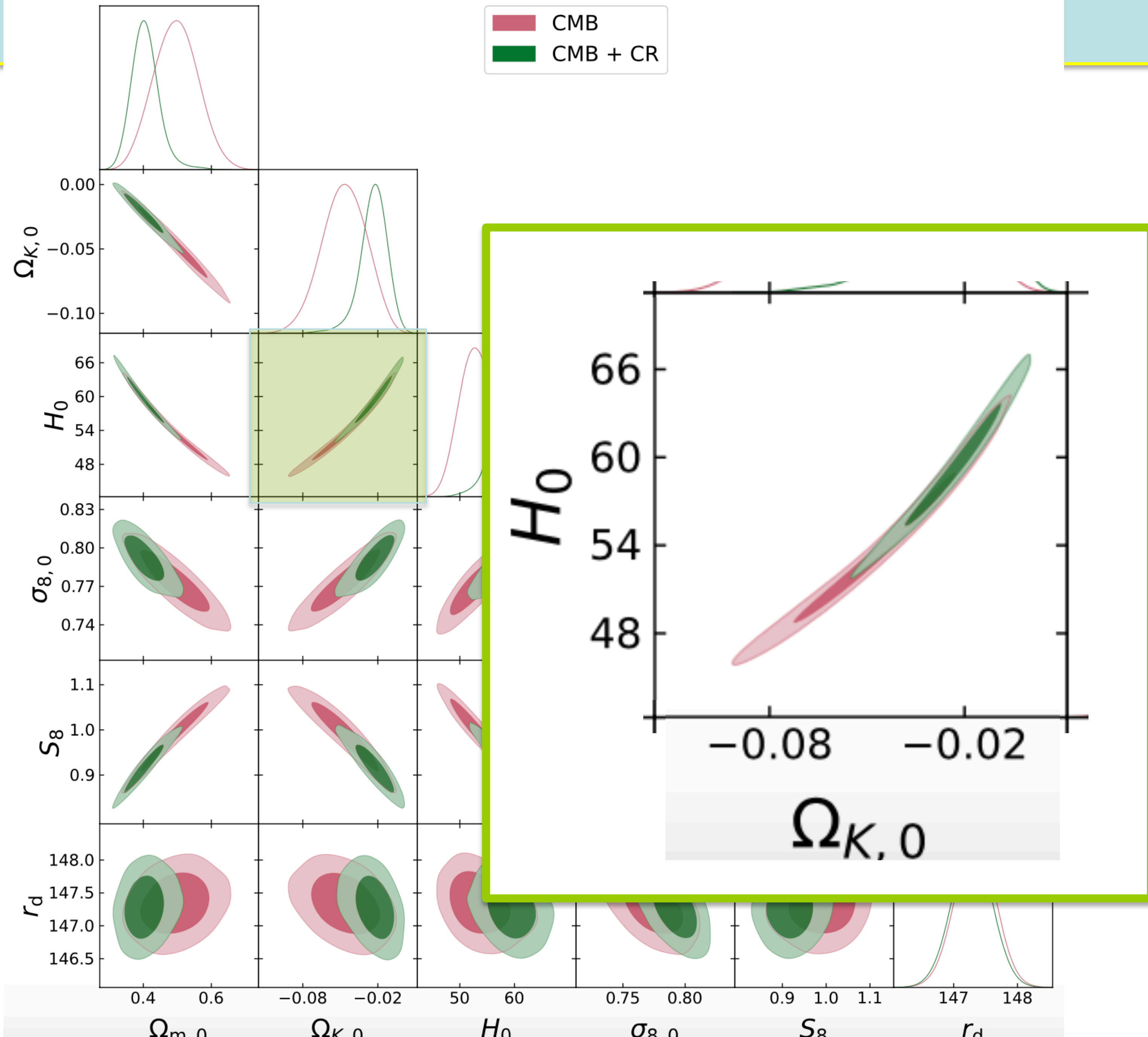

CMB
CMB + CR
$\Omega_{K,0}$
$H_0$
$\sigma_{8,0}$
$S_8$
$r_d$
$\Omega_{m,0}$
0.00
−0.05
−0.10
66
60
54
48
0.83
0.80
0.77
0.74
1.1
1.0
0.9
148.0
147.5
147.0
146.5
0.4
0.6
−0.08
−0.02
50
60
0.75
0.80
0.9
1.0
1.1
147
148

# Results

*The flat LCDM model cannot be rejected, there is a too high risk of rejecting the wrong model*

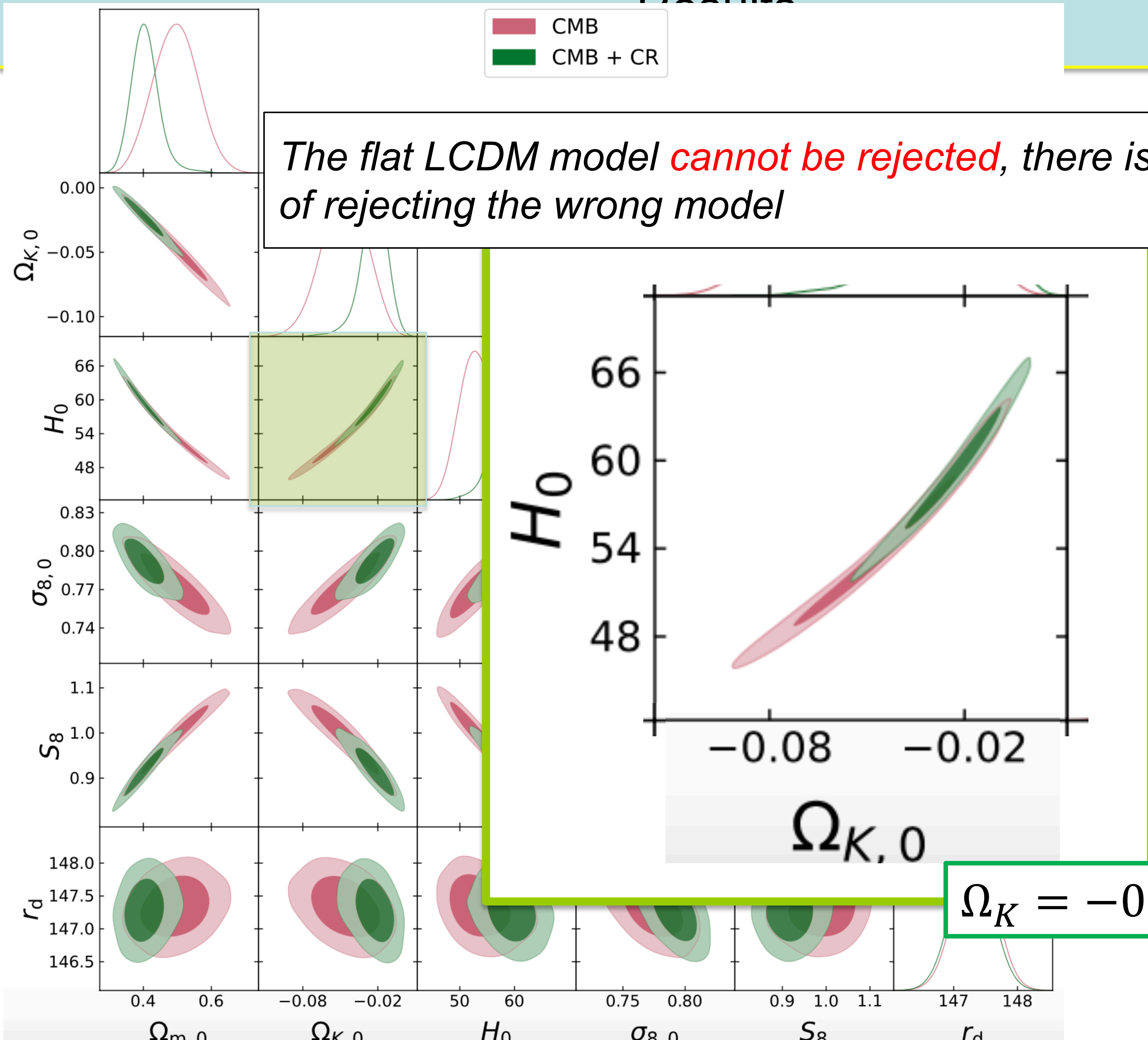


$$\Omega_K = -0.023 \pm 0.01$$

# Conclusions and Prospects

-Clustering alone (CR+RSD+BBN) allows to set a lower bound on $H_0$ ( > 62 km/s/Mpc at 95% C.L. )

-CR+RSD+BBN+BAO+SNIa allow to constrain curvature $\Omega_K = 0.004 \pm 0.05$

-According to DIC statistics the CR data do not disagree with CMB contrary to RSD and BAO it provides $\Omega_K = -0.023 \pm 0.01$ (cannot reject flatLCDM)

- CR+RSD+BBN+BAO+SNIa sound horizon $r_d = 144.57 \pm 2.34\ \mathrm{Mpc}$ compatible with CMB

- Master student (Mehdi Noor) will measure the CR in BOSS DR17 to extend the CR dataset

# Formalism in curved space

Statistical invariance: cross-correlation between Fourier modes:

$$\left\langle \delta_{lm}(\nu)\delta^*_{l'm'}(\nu')\right\rangle = \delta_{ll'}\,\delta_{mm'}\,\frac{\mathcal{S}(\nu)}{\nu^2}\begin{cases}\delta^{\mathrm{D}}(\nu-\nu') & \text{if} \quad K \leq 0,\\ \delta_{\nu\nu'} & \text{if} \quad K = 1.\end{cases}$$

-> There is no cross-correlation, only the power spectrum $\underline{\mathcal{S}(\nu)}$

$$\nu\,\mathcal{S}(\nu) = \frac{k}{a_0^2}\,P(k) \quad \text{where} \quad k = \frac{\tilde{k}}{a_0} = \frac{\sqrt{\nu^2 - K}}{a_0} \quad \text{and} \quad \tilde{k}\,\chi = k\,r.$$

Power spectrum:

$\mathcal{S}(\nu)$

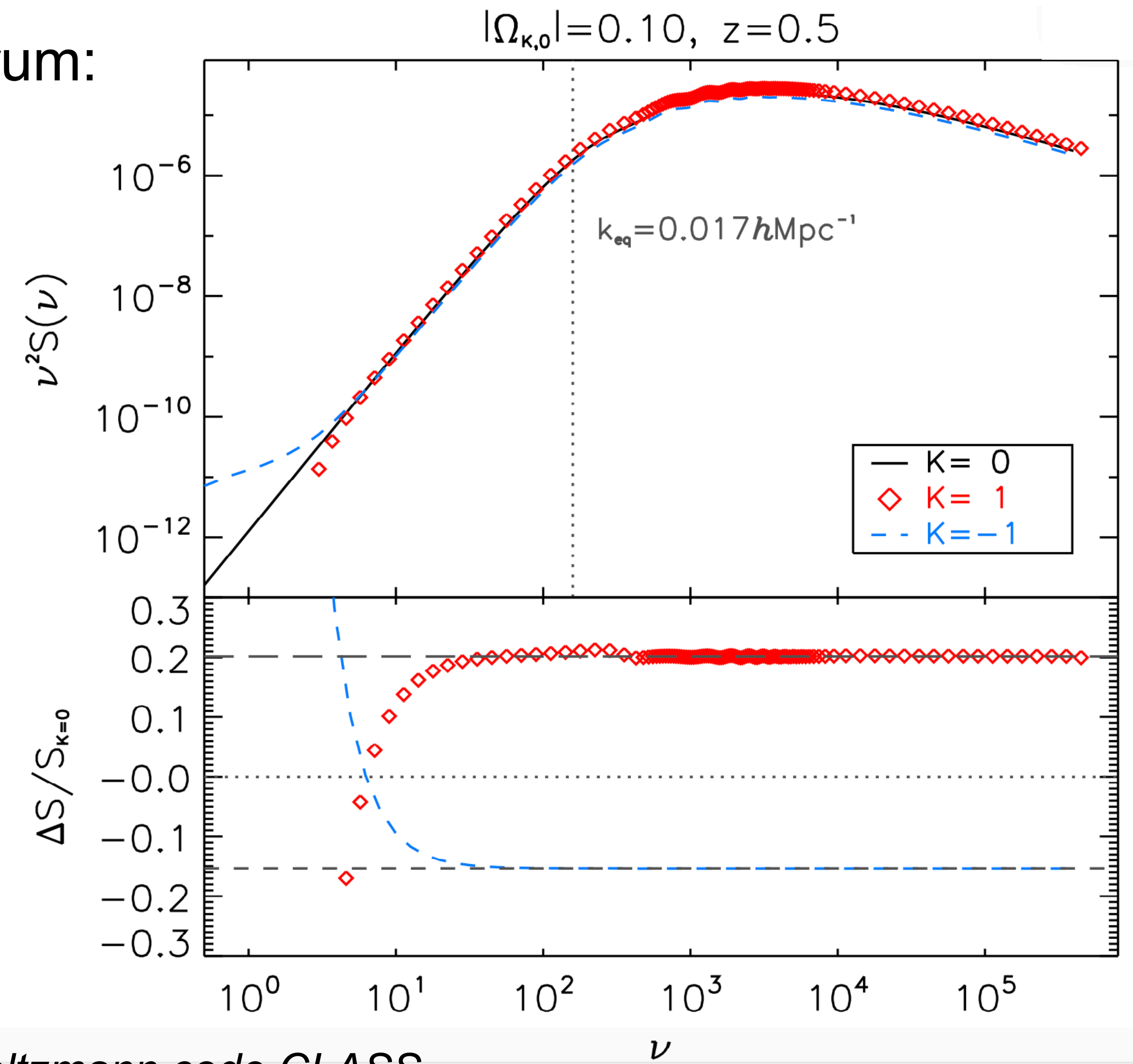


*Output from the Boltzmann code CLASS*

# Formalism in curved space

The matter, galaxy or halo density contrast can be expanded on the Fourier basis:

$$\delta(\chi, \theta, \phi) = 4\pi \int_0^\infty \mathrm{d}\nu\, \nu^2 \sum_{l=0}^{\infty} \sum_{m=-l}^{l} \delta_{lm}(\nu)\, \hat{X}_l^{(K)}(\nu, \chi)\, Y_{lm}(\theta, \phi),$$

where $\hat{X}_l^{(K)}(\nu, \chi)$ is the radial part of the Fourier basis and for convenience one can define the effective wave number $\nu$ as

$$\tilde{k}^2 = \nu^2 - K$$

The Fourier transform of the density contrast can be expressed

$$\delta_{lm}(\nu) = \frac{1}{2\pi^2} \int \mathrm{d}^2\Omega\, \mathrm{d}\chi\, S_K^2(\chi)\, \delta(\chi, \theta, \phi) \hat{X}_l^{(K)}(\nu, \chi) Y_{lm}^*(\theta, \phi)$$

# Galaxy clustering in configuration space

Multipole expansion of the 2-point correlation function:

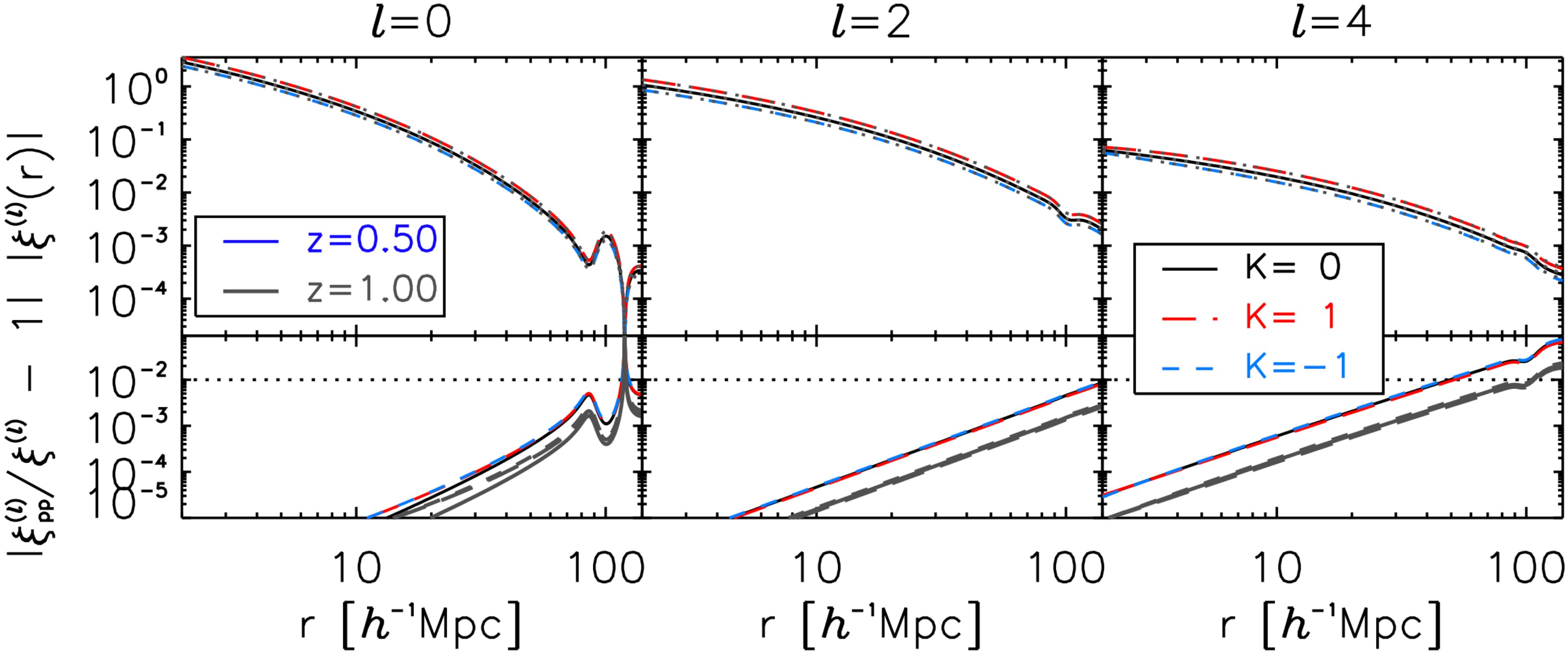


The hexadecapol is the most affected by **wide angle effects**

# Deviance Information Criterion (DIC)

Be D1 and D2 to data set, are those two data set in tension ?

$$DIC(D) = 2\overline{\chi^2_{eff}} - \chi^2_{eff} \quad \text{where} \quad \chi^2_{eff} = -2\ln\mathcal{L}_{max}$$

$\mathcal{L}_{max}$ is the maximum likelihood

$\overline{\chi^2_{eff}}$ average over the posterior

$$I(D_1, D_2) = \mathrm{e}^{-\mathcal{F}(D_1,D_2)/2} \quad \text{where } \mathcal{F}(D_1, D_2) = \mathrm{DIC}(D_1 \cup D_2) - \mathrm{DIC}(D_1) - \mathrm{DIC}(D_2)$$

If $\log_{10} I > 0$ there is agreement else there is disagreement

Jeffrey scale:

$|\log_{10} I| > 0.5$ -> *substantial*

$|\log_{10} I| > 1.0$ -> *strong*

$|\log_{10} I| > 2.0$ -> *decisive*

## 2-point correlation function density of pairs of object

$$\tilde{\xi}^s_{\rm g}(\tilde{r}, \tilde{\mu}) = \xi^s_{\rm g}(r, \mu)$$

where

$$r = \tilde{r}\,\alpha_\perp \left[1 + (\lambda^2 - 1)\,\tilde{\mu}^2\right]^{1/2}, \qquad \mu = \tilde{\mu}\,\lambda \left[1 + (\lambda^2 - 1)\,\tilde{\mu}^2\right]^{-1/2} \quad \text{where } \lambda = \frac{\alpha_\parallel}{\alpha_\perp}.$$

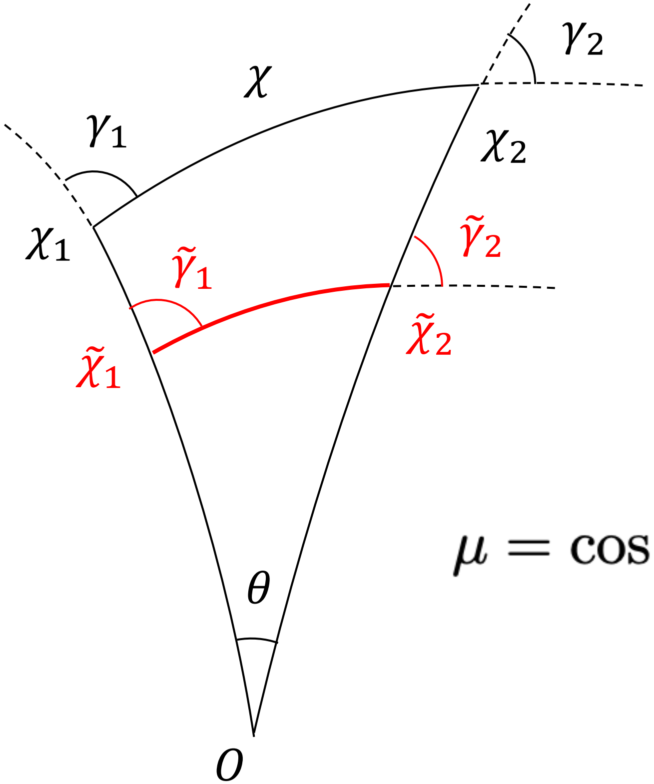


$$r_\parallel E(z) = \tilde{r}_\parallel \tilde{E}(z) \quad \Rightarrow \quad r_\parallel = \alpha_\parallel \tilde{r}_\parallel\,,$$

$$\frac{r_\perp}{D_A(z)} = \frac{\tilde{r}_\perp}{\tilde{D}_A(z)} \quad \Rightarrow \quad r_\perp = \alpha_\perp \tilde{r}_\perp\,,$$

$$\mu = \cos\gamma_1$$

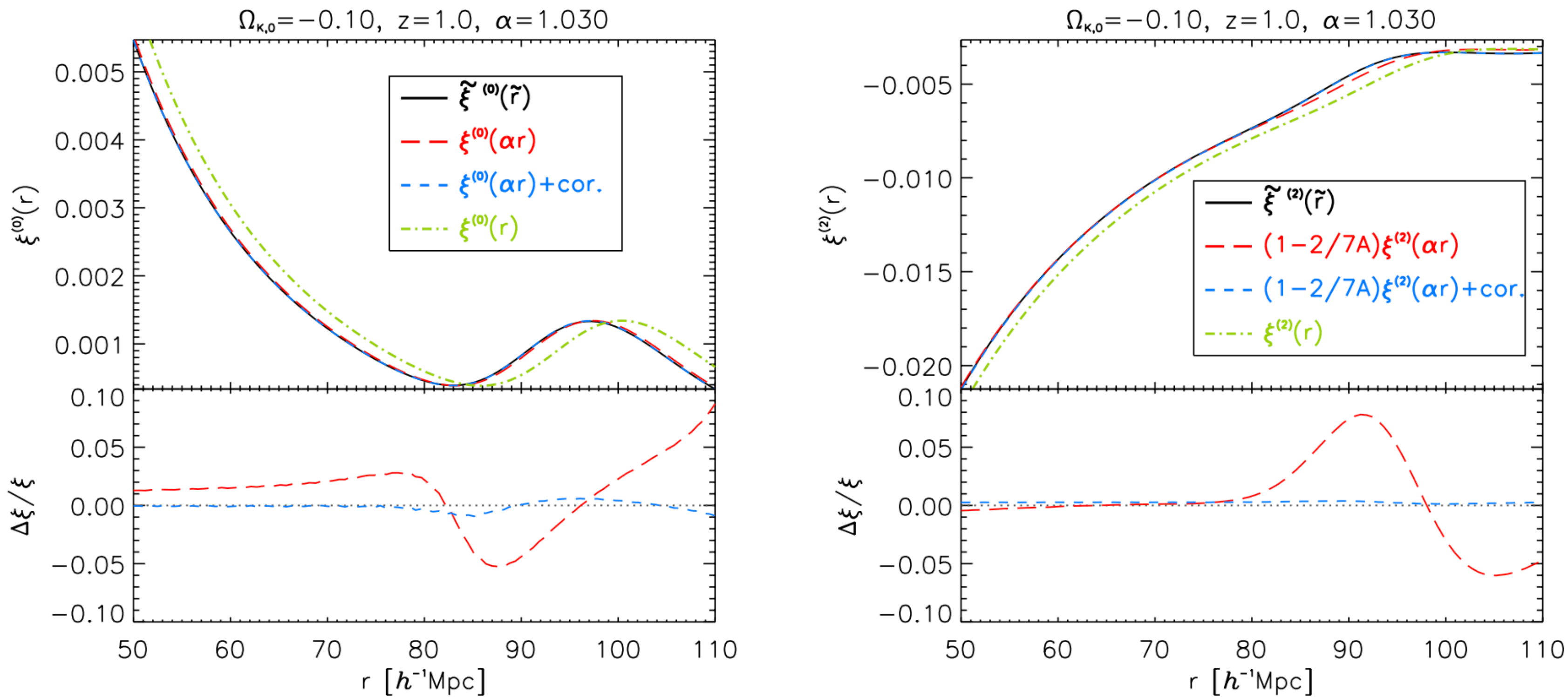


**Figure 12.** *Top:* AP effect on the monopole (A.16) (left) and quadrupole (A.18) (right). Solid black line shows the true distorted multipoles. Red long-dashed line shows the leading (first) contribution and blue short-dashed line is the correction. Green dot-dashed line shows the multipole without AP effect. Fiducial model: $\Omega_{\mathrm{m},0} = 0.37$, $\Omega_{K,0} = 0$; true model: $\Omega_{K,0} = -0.1$, $\Omega_{\mathrm{m},0} = 0.32$. *Bottom:* Fractional difference relative to true distorted multipoles.